

April 21, 2013 10:38

WSPC - Proceedings Trim Size: 9in x 6in Unpolarized\_Asym\_COMPASS

1

## MEASUREMENTS OF UNPOLARIZED AZIMUTHAL ASYMMETRIES AT COMPASS

W. Kafer on behalf of the COMPASS collaboration

Physikalisches Institut, Albert-Ludwigs-University Freiburg,  
79104 Freiburg, Germany  
E-mail: wolfgang.kaefer@ik.fzk.de

Azimuthal asymmetries in unpolarized SIDIS can be used to probe the transverse momentum of quarks inside the nucleon. Furthermore, they give access to the so-far unmeasured Boer-Mulders function. We report on the first measurement of azimuthal asymmetries of the SIDIS cross section from scattering of muons on a deuteron target.

Keywords: Deep Inelastic Scattering, DIS, Semi-inclusive Deep Inelastic Scattering, spin-independent azimuthal asymmetries, unpolarized Azimuthal Asymmetries, Cahn Effect, Boer-Mulders Effect, Boer-Mulders Function, COMPASS, CERN

### 1. Introduction and Theoretical Motivation

Semi-Inclusive Deep Inelastic Scattering (SIDIS) reactions are an important tool to probe the structure of the nucleon. Of particular interest in unpolarized SIDIS is a possible dependence of the cross section on the azimuthal angle of the hadron as defined in Fig. 1.

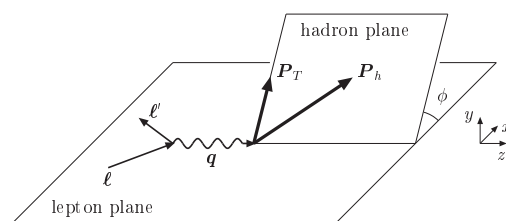


Fig. 1. Definition of the hadron azimuthal angle  $\phi_h$

There are several effects which contribute to a  $\cos \theta_h$  and  $\cos 2 \theta_h$  dependence of the cross section. The amplitudes of these modulations depend on the kinematic variables relevant for the SIDIS process, namely the Bjorken scaling variable  $x$ , the relative energy loss of the muon  $y$ , the negative 4-momentum of the virtual photon squared  $Q^2$ , the energy fraction of the hadron  $z$  and the transverse momentum of the hadron  $P_t^h$ . Furthermore,  $k_t$  is the transverse momentum of the quark with respect to the nucleon, and  $p_t$  the transverse momentum of the hadron with respect to the direction of the fragmenting quark.

The first azimuthal dependence discussed here is due to non-zero  $k_t$ : As Cahn pointed out in Ref. 5, an azimuthal modulation of the cross section is expected in one-photon exchange approximation, when the transverse momentum of the quark is taken into account. The Cahn effect contributes to a possible  $\cos \theta_h$  and  $\cos 2 \theta_h$  asymmetry of the SIDIS cross section. It is kinematically suppressed by  $\frac{k_t}{Q}$  for  $\cos(\theta_q)$  and  $\frac{k_t^2}{Q^2}$  for the  $\cos 2 \theta_q$  term. When going from the quark to hadron level, the unpolarized parton distribution functions (PDFs)  $f_q(x; k_t)$  and fragmentation functions (FFs)  $D_q^h(z; p_t)$  need to be taken into account. Assuming Gaussian distributions for the transverse momentum dependence of  $f_q(x; k_t)$  and  $D_q^h(z; p_t)$  and introducing  $D_{\cos \theta_h}(y) = \frac{(2-y)^p 1-y}{1+(1+y)^2}$ , the  $\cos \theta_h$  term can be written as

$$\frac{d^5}{dx dy dz dP_t^h d\theta_h} \int_{-X}^X f_q(x) D_q^h(z) \frac{1}{Q} \frac{hk_t^2 iz P_t^h}{h P_t^h} \cos \theta_h : \quad (1)$$

The  $\cos \theta_h$  modulation allows the determination of  $hk_t^2$ . This has been done e.g. in Ref. 6 using results from previous experiments, arriving at  $hk_t^2 = 0.25 \text{ GeV}^2/c^2$ .

The second contribution to azimuthal asymmetries comes from the Boer-Mulders PDF  $h_1^T(x; k_t)$ , convoluted with the Collins FF  $H_1^T(x; p_t)$ . A model calculation<sup>8</sup> shows that the Boer-Mulders contribution to the  $\cos 2 \theta_h$  modulation might be of similar magnitude than the contribution from the Cahn effect. In particular, a possible difference between positive and negative hadron asymmetries could be explained by the Boer-Mulders mechanism. It may also contribute to the  $\cos \theta_h$  asymmetry,<sup>7</sup> but the size of this effect is so far unknown and no predictions exist.

Perturbative QCD (pQCD) introduces a third  $\theta_h$  dependence at order  $\alpha_s$ . However, QCD effects are only important at  $P_t^h > 1 \text{ GeV}/c$ . Therefore they are expected to be small for COMPASS kinematics, where most of the statistics is at low transverse momentum. The perturbative contribution

has been given in Refs. 9,10 at  $O(\frac{1}{s})$ . Recently, higher order contributions were calculated in Ref. 11.

Since the muon beam used at the COMPASS experiment is naturally polarized, an additional modulation of the cross section is expected. In contrast to the Cahn, Boer-Mulders and pQCD contributions, the cross section for the beam asymmetry depends on  $\sin^2 \theta_h$ .<sup>12</sup> This effect has recently been measured by the CLAS collaboration<sup>13</sup> on a proton target.

Radiative corrections and possible higher twist terms may contribute to the modulations, but these effects are considered to be small and therefore will not be discussed here.

The overall cross section for SIDIS on an unpolarized target is thus of the form :

$$\frac{d}{d_h} / 1 + A_{\cos \theta_h} \cos \theta_h + A_{\cos^2 \theta_h} \cos^2 \theta_h + A_{\sin \theta_h} \sin \theta_h : \quad (2)$$

The amplitudes of these three modulations have been determined from data taken with the COMPASS experiment with a deuteron target.

For a proton target, three experiments have published results on azimuthal asymmetries in different kinematic regions: EMC,<sup>1,2</sup> the E665 collaboration<sup>3</sup> and the ZEUS experiment<sup>4</sup>.

## 2. The COMPASS Experiment

The COMPASS experiment<sup>14</sup> is a fixed target experiment at CERN. It features a 160 GeV/c<sup>+</sup> beam, with a natural polarization of -80% and a polarized target, which consists of two cells. From 2002-2006, data was taken with a polarized <sup>6</sup>LiD target, while in 2007 a hydrogen target was used. The target can be polarized either in the longitudinal or the transverse direction with respect to the beam direction. These two configurations will be called CL and CT in the following.

The different magnetic fields needed to maintain the target polarization (a solenoid field for CL and a dipole field for CT), require changes of the magnetic configuration of the experiment. In particular, the beam line settings differ, since an additional kick is needed for the CT setup to compensate the additional dipole field. On the other hand, for CL, there is a strong interference between the target magnetic field and the magnetic field of the first spectrometer magnet, which is not present for CT.

### 3. Asymmetry Extraction

The data sample used for this analysis was taken in the year 2004. Data samples in both target configurations (CL and CT) have been used in order to get a better estimate of the systematic error generated by experimental conditions.

The final sample consists of about 5 million positive and 4 million negative hadrons in the kinematic range  $Q^2 > 1 \text{ GeV}^2/c^2$ ,  $0.1 < y < 0.9$ ,  $0.2 < z < 0.85$  and  $0.1 \text{ GeV}/c < P_t^h < 1.5 \text{ GeV}/c$  and contains data from both target configurations in roughly equal parts. The target polarization was canceled by event weighting, taking into account the fluxes and average polarizations:

$$N_{\text{unpol}} = P_2 N_1 + F P_1 N_2 \quad (3)$$

where  $P_i$  indicates the absolute value of the polarizations for the two possible spin configurations ( $+$ ;  $-$  for CL and  $+$ ;  $+$  for CT),  $N_i$  the event number for the respective polarization and  $F = \frac{F_1}{F_2}$  the corresponding ratio of the respective muon fluxes.

In order to correct for event losses caused by the non-uniform acceptance of the COMPASS spectrometer, full MC simulations have been performed in both CL and CT setup. In each case, the events were generated with LEPTO, transported through the COMPASS detector simulation program COMGEANT and the reconstruction software CORAL. From these MC samples, the acceptance of the COMPASS spectrometer  $A(\theta_h)$  and the corrected count rates  $N_{\text{corr}}(\theta_h)$  can be determined:

$$A(\theta_h) = \frac{N_{\text{rec}}(\theta_h)}{N_{\text{gen}}(\theta_h)} \quad N_{\text{corr}}(\theta_h) = \frac{N_{\text{unpol}}(\theta_h)}{A(\theta_h)} \quad (4)$$

The acceptance correction has been done in bins of  $x$ ;  $z$ , and  $P_t^h$  separately, with the other two variables always integrated out. Fig. 2 shows a typical example of measured  $\theta_h$  distribution and the corresponding acceptance. The corrected count rates are then fitted with a four-parameter fit containing the average count rate  $N_0$  and the three amplitudes:

$$N_{\text{corr}} = N_0 (1 + A_{\sin \theta_h} \sin \theta_h + A_{\cos \theta_h} \cos \theta_h + A_{\cos 2 \theta_h} \cos 2 \theta_h) \quad (5)$$

### 4. Results

The amplitudes  $A_{\cos \theta_h}$ ;  $A_{\cos 2 \theta_h}$  and  $A_{\sin \theta_h}$  of the three modulations have been determined in dependence on  $x$ ;  $z$  and  $P_t^h$  for positive and negative hadrons separately. Fig. 3 shows the results for the three modulations for

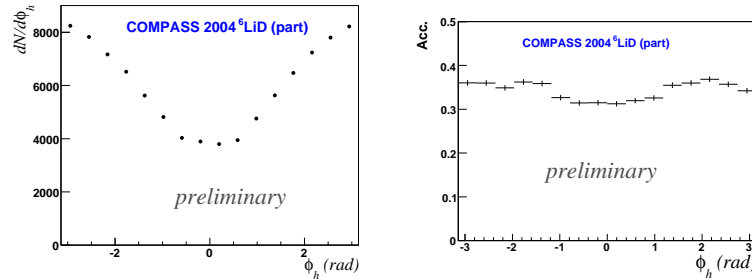


Fig. 2. Measured  $\phi_h$  distribution before correction and acceptance in the CT case for  $0.63 < z < 0.85$ .

positive hadrons. A large  $\cos \phi_h$  amplitude of up to 40% and a  $\cos 2 \phi_h$  amplitude of up to 5% is seen. The value for  $A_{\sin \phi_h}$  are consistent with zero. Also for the negative hadrons, shown in Fig. 4, the  $\sin \phi_h$  amplitude is consistent with zero, while the two cosine amplitudes show similar trends compared to the positive hadrons. However, the magnitude of the cosine modulations differs significantly for positive and negative hadrons.

Fig. 5 shows a recent prediction<sup>15</sup> for a deuteron target and the COMPASS kinematics, compared to the data. Only Cahn and perturbative QCD contributions have been considered. Calculation and data show similar behaviour in the region of large  $x$ , while there is disagreement in the region of small  $x$ . The strong disagreement in the low  $x$  region leads to a scale difference in  $z$ , although the slope, which is mainly due to the Cahn Effect, is again similar. A model-calculation<sup>8</sup> for the  $\cos 2 \phi_h$  amplitude is compared to the COMPASS results in Fig. 6. Here also the Boer-Mulders mechanism has been included. Since  $h_1^2(x; k_t)$  is presently not constrained by experimental data, it has been assumed to be proportional to the better known Sivers function. This assumption has e.g. been motivated in Ref. 16.

## 5. Systematic tests

Several checks have been performed to determine the systematic error of the measurement. It turns out that the systematic error is due to two sources: the difference between the results in the setups CL and CT and the variation of the acceptance for different generated kinematic distributions. These differences are used as an estimate for the quality of the acceptance correction. To evaluate the second contribution, for each setup, CL and CT, two MC simulations with different LEPTO settings and thus different generated kinematic distributions have been performed. Several additional tests,

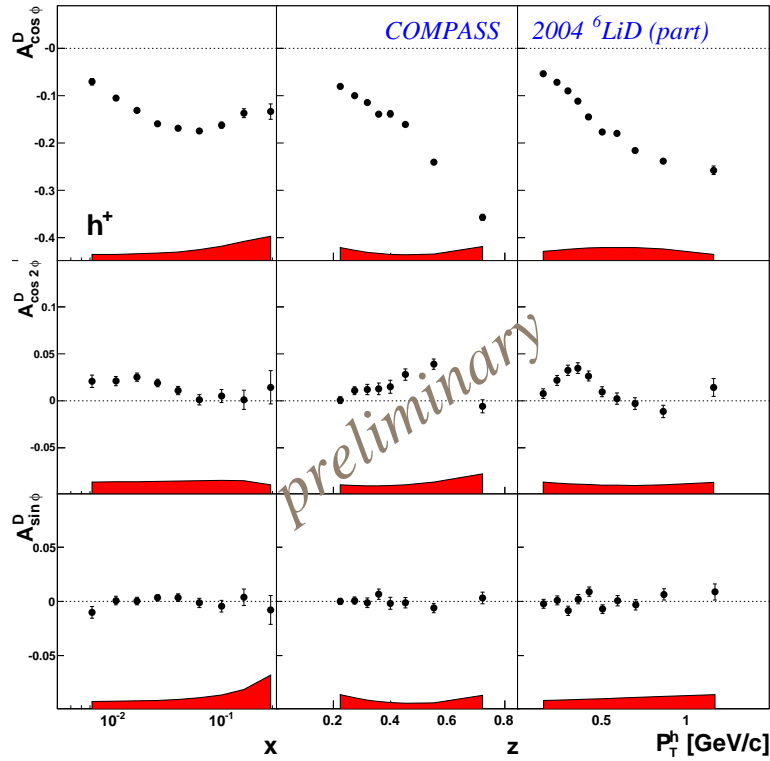


Fig. 3. Results for positive hadrons for  $A_{\cos \phi}^D$ ,  $A_{\cos 2 \phi}^D$  and  $A_{\sin \phi}^D$  in dependence of the kinematic variables  $x$ ;  $z$ ;  $P_T^h$ . The error bars correspond to the statistical errors, while the error bands at the bottom indicate systematic errors.

such as splitting the data sample according to the event topology, target polarization and time of the measurement give no significant contribution to the systematic error.

### 6. Summary and Outlook

First results on unpolarized azimuthal asymmetries from COMPASS have been presented, extending the investigated kinematic region to low  $x$ . The data can be used to better determine the value of  $hk_t^2$ . Also the differences between positive and negative hadrons allow to gain knowledge about  $h_1^2(x; k_t)$ , which can be further deepened with the data taken in 2007 with a  $NH_3$  target.

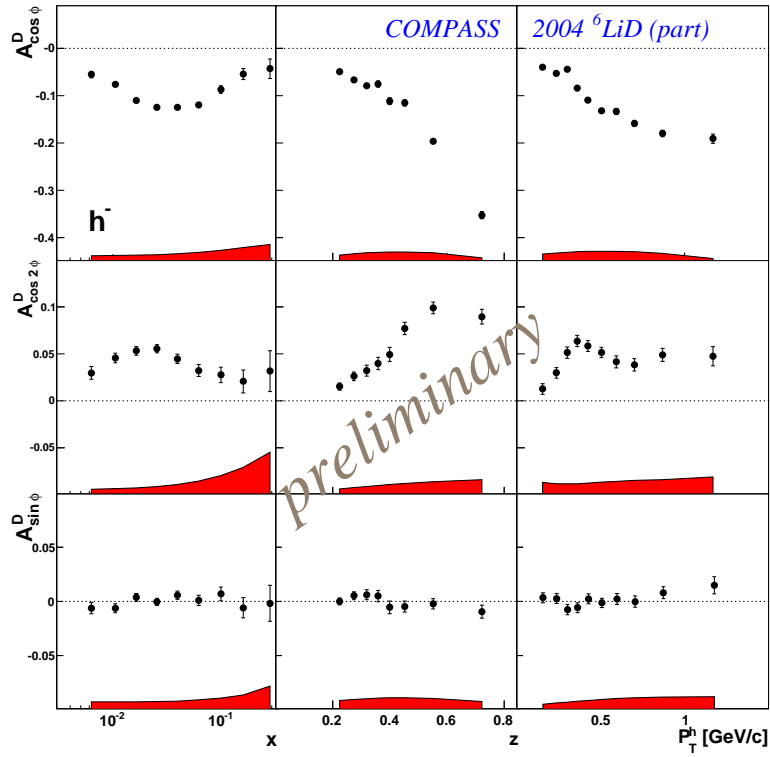


Fig. 4. Results for negative hadrons for  $A_{\cos \phi}^D$ ,  $A_{\cos 2 \phi}^D$  and  $A_{\sin \phi}^D$  in dependence of the kinematic variables  $x$ ;  $z$ ;  $P_T^h$ . The meaning of the error bars and bands is the same as in the previous figure.

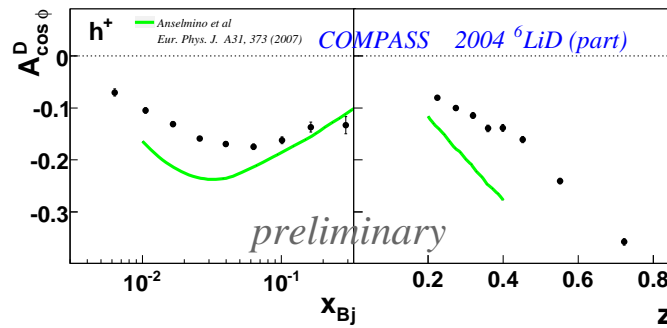


Fig. 5. Comparison of  $A_{\cos \phi}^D$  for positive hadrons with model calculation from Ref. 15, which takes into account Cahm and perturbative QCD effects. Only statistical errors are shown.

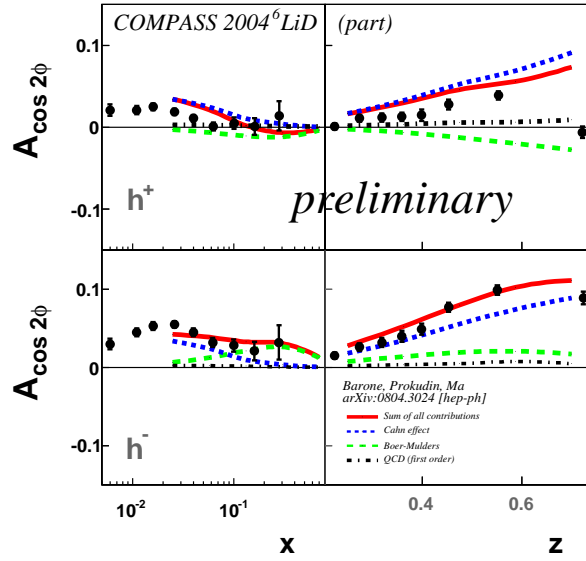


Fig. 6. Comparison of  $A_{\cos 2\phi}$  with predictions for COMPASS kinematics from Ref. 8. The calculation takes into account the Cahn effect (dashed curve), perturbative QCD (dashed dotted) and Boer-Mulders (dotted curve). The continuous line describes the sum of these three. A gain, only statistical errors are shown.

## References

1. European Muon Collaboration, *Phys. Lett. B* 130, 118 (1983).
2. European Muon Collaboration, *Z. Phys. C* 34, 277 (1987).
3. E665 Collaboration, *Phys. Rev. D* 48, 5057 (1993).
4. ZEUS Collaboration, *Phys. Lett. B* 481, 199 (2000).
5. R. N. Cahn, *Phys. Lett. B* 78, 269 (1978).
6. M. Anselmino et al., *Phys. Rev. D* 71, 074006 (2005).
7. D. Boer and P. J. Mulders, *Phys. Rev. D* 57, 5780 (1998).
8. V. Barone, A. Prokudin and B. Q. Ma, *Phys. Rev. D* (2008), accepted for publication, arXiv:0804.3024 [hep-ph].
9. H. Georgi and H. D. Politzer, *Phys. Rev. Lett.* 40, 3 (1978).
10. A. Mendez, *Nucl. Phys. B* 145, 199 (1978).
11. A. Daleo, D. de Florian and R. Sassot, *Phys. Rev. D* 71, 023013 (2005).
12. A. Kotzinian, *Nuclear Physics B* 441, 234 (1995).
13. CLAS Collaboration, *Phys. Rev. D* 69, 112004 (2004).
14. COMPASS Collaboration, *Nucl. Instr. Meth.* 577, 455 (2007).
15. M. Anselmino et al., *Eur. Phys. J. A* 31, 373 (2007).
16. M. Burkardt, *Phys. Rev. D* 72, 094020 (2005).